Monthly Notices
of the
ROYAL ASTRONOMICAL SOCIETY

Mon. Not. R. Astron. Soc. **412,** 1361–1366 (2011) doi:10.1111/j.1365-2966.2010.17996.x

An analysis of the blue straggler population in the Sgr dSph globular cluster Arp 2⋆

Giovanni Carraro[1]†‡ and Anton F. Seleznev[2]‡

[1]*European Southern Observatory, Alonso de Cordova 3107, Casilla 19001, Santiago 19, Chile*
[2]*Astronomical Observatory, Ural State University, Lenin Avenue, 51, Ekaterinburg 620083, Russia*

Accepted 2010 November 6. Received 2010 November 5; in original form 2010 September 7

ABSTRACT

We present and discuss new *BVI* CCD photometry in the field of the globular cluster Arp 2, which is considered a member of the Sagittarius dwarf spheroidal galaxy. The main goal of this investigation is to study the statistics and spatial distribution of blue straggler stars in the cluster. Blue stragglers are stars observed to be hotter and bluer than other stars with the same luminosity in their environments. As such, they appear to be much younger than the rest of the stellar population. Two main channels have been suggested to produce such stars: (1) collisions between stars in clusters; or (2) mass transfer between, or merger of, the components of primordial short-period binaries. The spatial distribution of these stars inside a star cluster, compared with the distribution of stars in different evolutionary stages, can cast light on the most efficient production mechanism at work. In the case of Arp 2, we found that blue straggler stars are significantly more concentrated than main-sequence stars, while they show the same degree of concentration as evolved stars (either red giants or horizontal branch stars). Since Arp 2 is not a very concentrated cluster, we suggest that this high central concentration is an indication that blue stragglers are mostly primordial binary stars.

Key words: binaries: general – blue stragglers – stars: evolution – open clusters and associations: general – open clusters and associations: individual: Arp 2.

1 INTRODUCTION

Arp 2 is a globular cluster located at $l = 8.^{\circ}54$, $b = -20.^{\circ}78$ ($\alpha = 19^{h}28^{m}44^{s}$, $\delta = -30^{\circ}21'14''$, J2000.0). It is commonly believed to have formed inside the Sgr dwarf spheroidal galaxy (Monaco et al. 2005), and then been released into the Milky Way through tidal interaction. With a metallicity of [Fe/H] = −1.77 (Mottini, Wallerstein & McWilliam 2008), this cluster appears to be 3–4 Gyr younger than the old globulars, but ∼1–2 Gyr older than the youngest globulars associated with Sgr (Layden & Sarajedini 2000; Carraro, Zinn & Moni Bidin 2007). The first photometric study of this cluster was performed by Buonanno et al. (1994). The colour–magnitude diagram (CMD) these authors derived reveals an intriguing feature, namely that the horizontal branch (HB) is located entirely blueward of the RR Lyrae instability strip, a fact that allowed the authors to assess its age through a differential comparison with 47 Tuc and Ruprecht 106. A secondary, prominent feature, which the authors do not comment on, is a group of stars right above the turn-off (TO), which are probably the blue straggler star (BSS) population in Arp 2. BSSs are a normal stellar population in clusters, since they are present in all of the properly observed globular clusters (GCs, Ferraro 2006; Ferraro et al. 2009, and references therein). The current scenario for these stars in globulars is that they are either binary systems with significant mass exchange, or stellar mergers resulting from direct collisions between two or more stars (Davies, Piotto & de Angeli 2004; Knigge, Leigh & Sills 2009; Perets & Fabrycky 2009).

In all these studies a proper assessment of the membership of BSSs through comparison with red giant branch (RGB) stars was routinely performed (Ferraro et al. 1993). That they are compared for their cumulative radial distribution may hint at their possible common origin, specifically to confirm whether or not they belong to the same parent distribution.

Additionally, the radial distribution of BSSs in a star cluster is the most effective tool to understand their origin and their dominant production channel (Ferraro 2006). BSSs are routinely found – with the exception of Omega Cen and NGC 2419 (Dalessandro et al. 2008a) – to be centrally concentrated. Their radial profile then smooths down, while in the cluster periphery it shows again an increase in the BSS contribution (Lanzoni et al. 2007; Dalessandro et al. 2008b).

In this paper we report on a new photometric data set of Arp 2 obtained with the goal of analysing the BSS population in a young, relatively loose GC that is in an environment significantly different

⋆Based on observations carried out at ESO La Silla under programme 081.C-0087(A).

†On leave from Dipartimento di Astronomia, Università di Padova, Italy.
‡E-mail: gcarraro@eso.org (GC); anton.seleznev@usu.ru (AFS)

from a typically dense GC. We anticipate here that our analysis reveals that BSSs in Arp 2 do share the same distribution of RGB and horizontal branch (HB) stars, and are more concentrated than main sequence (MS) stars.

This paper is organized as follows. In Section 2 we illustrate how we collected and analysed our data, while in Section 3 we present the star counts in Arp 2 to measure its size. The CMD of Arp 2 is presented and discussed in Section 4, whereas the definition of BSSs, and their statistics, is discussed in Section 6, where we also comment on and summarize our findings.

2 OBSERVATIONS AND DATA REDUCTION

CCD *BVI* images were acquired with the EFOSC2 camera mounted on the Nasmyth focus of the ESO NTT telescope on the night of 2008 August 8. The CCD is a 1030 × 1038 array with a scale of 0.24 arcsec, allowing us to cover 4.1 × 4.1 arcmin^2 on the sky. This allowed us to cover a field centred on Arp 2 and slightly larger than the previous observations by Buonanno et al. (1994). We used multiple exposures for 30 and 1200 s for the *B* filter, and for 30 and 900 s each for *V* and *I* filters. As an illustration, a 900-s raw image taken with an *I* filter is shown in Fig. 1. The night was photometric, and we calibrated our photometry against the Landolt (1992) standard field Mark A and PG 2213, observed several times during the night. Arp 2 was observed during an observational run focused on different science when the principal target was not visible. Data have been reduced in the standard way. Image preparation (trimming, bias and flat-field) was done using the IRAF package, while photometry was extracted by using DAOPHOT and ALLSTAR (Stetson 1987). We obtained a final catalogue with 4580 entries having 2000.0 equatorial coordinates and *B*, *V* and *I* magnitudes together with associated uncertainties. We calculated these magnitudes using the method of Patat & Carraro (2001).

2.1 Complementary infrared data, astrometry and completeness

Our optical catalogue was cross-correlated with 2MASS, which resulted in a final catalogue including *BVI* and JHK_s magnitudes.

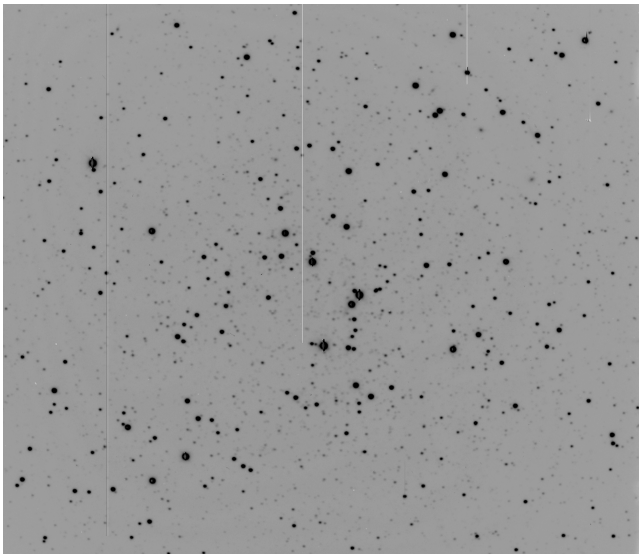

Figure 1. A raw 900-s image in the *I* filter of Arp 2. North is up, east to the left, and the field of view is ∼4 arcmin on a side.

As a by-product, pixel (detector) coordinates were converted to RA and Dec. for J2000.0 equinox, thus providing 2MASS-based astrometry.

Finally, completeness corrections were determined by running artificial star experiments on the data. The data set was divided into two regions, inner (1 arcmin or less) and outer (beyond 1 arcmin), and completeness was computed for these two different regions, which, due to the nature of the object, are expected to be differently affected by star crowding (Carraro et al. 2007). Basically, we created several artificial images by adding artificial stars to the original frames. These stars were added at random positions, and had the same colour and luminosity distribution as the true sample. To avoid generating overcrowding, in each experiment we added up to 30 per cent of the original number of stars. Depending on the frame (short or deep exposures), between 1000 and 5000 stars were added. In this way we have estimated that the completeness level of our photometry in the outer region is 100 per cent down to $V = 23.00$, and better than 50 per cent down to $V = 23.50$. As for the inner region, we found that the completeness is 100 per cent down to $V = 22.40$, and better than 50 per cent down to $V = 22.80$.

3 STAR COUNTS AND CLUSTER SIZE

We used our photometry to study the cluster stars' radial distribution. According to Harris (1996), Arp 2 has a concentration *c* of 0.90, a half-mass radius of 1.91 arcmin, and core and tidal radius of 1.59 and 12.65 arcmin, respectively. Therefore, we expect our photometry to cover just the inner part of the cluster. The radial density profile we constructed is shown in Fig. 2. It has been derived following the method described in Seleznev (1994). This method employs numerical differentiation of the best mean-square polynomial fit for $N(r)$, the number of stars in circles of radius r in the plane of the sky. The centre of the cluster was taken at the detector coordinates (512, 512) which corresponds to $\alpha = 19^{\rm h}28^{\rm m}44^{\rm s}$, $\delta = -30^\circ21'14''$ (J2000.0). Vertical bars indicate the profile error bars derived assuming Poisson statistics. In the same Fig. 2 we fit the profile with a King (1962) model, adopting King parameters (core and tidal radius, and centre mass density) from Harris's (1996) compilation. The fit is good within the uncertainties, and therefore we conclude that Arp 2 follows a King-like density profile. It decreases all the

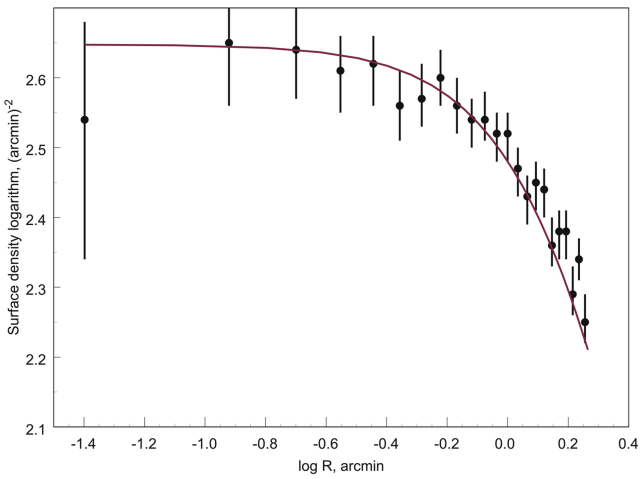

Figure 2. Radial surface density profile as derived from our photometry. Superimposed is a fit with a King profile, drawn adopting Harris (1996) parameters.

way to the edge of the field we covered, slightly beyond the nominal half-mass radius.

4 COLOUR–MAGNITUDE DIAGRAMS

The resulting CMDs are shown in the two panels of Fig. 3. In the left-hand panel, the V versus $B - V$ diagram is shown, while in the right-hand panel we present V versus $V - I$. The CMD in the left-hand panel is absolutely identical to the one presented by Buonanno et al. (1994), apart from the slightly different area coverage and the magnitude limit, which in our case is about 1 magnitude fainter. All the typical features of a globular cluster CMD are present: the MS, RGB, HB – located entirely blueward of the RR Lyrae instability strip – and the asymptotic giant branch (AGB). An additional feature that has been overlooked in the past is the plume of blue stars right above the turn-off (TO) point, which is quite common in globular clusters, and it is composed of candidate blue straggler stars. This plume is the target of our investigation. We look for BSS candidates following the commonly used criteria (Sandage 1953; Ahumada & Lapasset 1995, 2007) that we have illustrated in Fig. 4. Together with the BSS (blue box), we have also indicated the location of the HB (red box), RGB (red dots) and a sample of MS stars (yellow box), which we are going to compare. We counted 41 BSS candidates and 28 HB stars. We list them in Tables 1 and 2, respectively, where we indicate the stars' identification (our numbering, ID), the equatorial coordinates for the 2000.0 equinox, the magnitude V and the colour $B - V$. These can also be useful for future spectroscopic follow-up studies.

Besides, again from Fig. 4, we counted 213 RGB and 517 MS stars, but we do not list them in this paper to save space. As for MS stars, we stress that they have been extracted in a region of the MS which is not affected by incompleteness.

We stress that the numbers we report have been computed using the classical definition of BSS locus and assuming that contamination from field stars is negligible, which seems to be the case, since the field of view is very small (0.0044 deg^2). However, we do not have at our disposal a control field to verify this directly. Therefore, we investigated the amount of contamination by computing synthetic CMDs of stars in the direction of Arp 2 assuming a Galactic model which includes bulge, halo, thin and thick discs (Girardi et al. 2005). We generated several CMDs by varying the random seed, and we added photometric errors as from Arp 2 photometry. The results

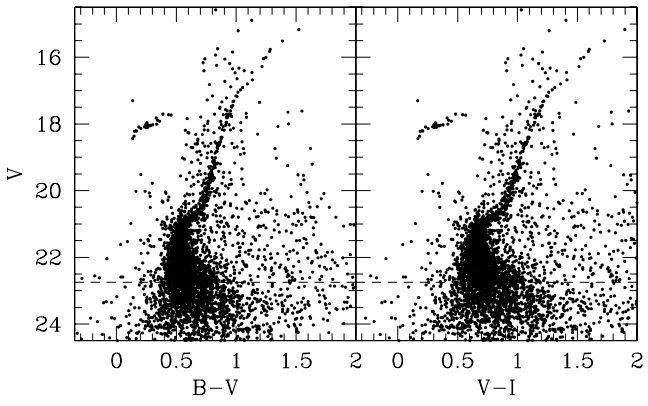

Figure 3. CMDs in V versus $B - V$ (left-hand panel) and V versus $V - I$ (right-hand panel) for Arp 2. The dashed lines indicate the 100 per cent level of completeness. See Section 2.1.

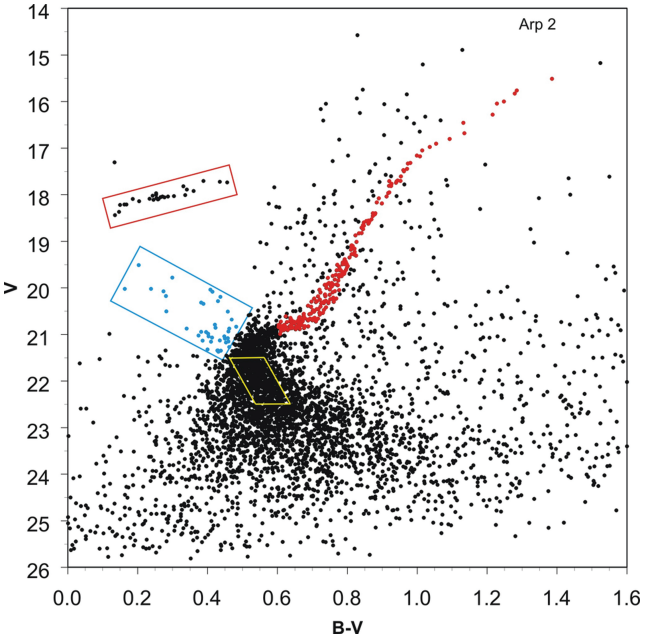

Figure 4. Selection of RGB (red dots), HB (red box), BSS (blue box) and MS (yellow box) stars. The last ones have been selected in a region of the MS where the completeness is 100 per cent.

are shown in Fig. 5, where the left-hand panel shows the Galaxy CMD in the direction of Arp 2, and the right-hand panel shows the CMD of Arp 2 as in Fig. 4. In both panels we indicate the boxes used for selecting HB (red) and BSS (blue) stars. A quick glance at this figure is sufficient to conclude that most of the contamination affects the lower MS, and in general contaminating stars are redder than the typical BSS colours. Some contamination is present in the RGB area but, given the high number of RGB stars in Arp 2, we do not expect their statistics to be significantly affected.

5 ANALYSIS OF THE BLUE STRAGGLER STAR POPULATION

To properly assess the probable membership of BSSs, it is necessary to measure either their radial velocity or their proper motion (Liu et al. 2008; Mathieu & Gheller 2009). Since we are relying only on photometry, we will stick to considering our BSSs as candidates, based on their location in the CMD. To get more insight into their properties and origin, we started by considering their surface distribution, and compared it with the surface distribution of HB stars. This is illustrated in Fig. 6, which shows the radial density profiles of the two populations. In this figure we plot the number of stars per arcmin^2 as computed in 10-arcsec wide concentric bins. Except for the difference in the inner side of the cluster, the two profiles are identical. We stress that the difference in the central-most bin, although real, is inflated by the small-number statistics (2 BSS and 0 HB stars). In this respect Arp 2 seems more similar to old open clusters, like M67 (Mathieu & Gheller 2009), than to genuine globulars. The higher concentration of BSSs that we find in the cluster internal region with respect to the evolved stars is not new information, and has already been found in several other globulars (Dalessandro et al. 2008b). At odds with what is found in other globulars, we do not see any outward increase of the BSS population, most probably because we are not sampling the cluster outskirts (see Section 3) in this study.

Table 1. BSS candidates. See Fig. 4 for the selection.

ID	α (2000.0)	δ(2000.0)	V	$B-V$
140	292.146 3587	−30.339 4516	19.777	0.299
742	292.153 9322	−30.357 4441	21.321	0.400
909	292.156 0467	−30.359 0792	20.831	0.482
1086	292.158 4272	−30.359 0217	21.173	0.453
1119	292.159 0122	−30.340 4261	20.071	0.274
1463	292.162 7267	−30.354 4101	20.191	0.437
1575	292.163 9108	−30.367 6803	21.347	0.438
1649	292.164 9792	−30.356 5927	21.040	0.448
1942	292.168 1176	−30.377 0277	20.871	0.340
2257	292.171 8385	−30.356 4573	20.680	0.469
2308	292.172 3293	−30.357 0290	20.282	0.430
2324	292.172 7334	−30.340 9102	20.315	0.382
2341	292.172 5939	−30.358 8043	21.154	0.410
2433	292.174 1541	−30.320 8680	20.853	0.423
2531	292.174 3077	−30.379 0334	21.371	0.431
2568	292.174 8233	−30.372 2961	21.268	0.462
2750	292.177 0090	−30.347 0938	21.341	0.430
2826	292.177 9222	−30.338 6991	21.040	0.403
2910	292.178 2726	−30.379 5017	21.024	0.374
2913	292.178 8245	−30.343 2700	20.935	0.460
3146	292.181 0024	−30.357 3719	20.947	0.396
3163	292.181 5525	−30.332 2570	20.343	0.388
3266	292.182 2050	−30.351 9277	21.131	0.386
3351	292.182 9014	−30.366 2331	20.172	0.281
3362	292.183 0748	−30.359 8515	20.039	0.408
3533	292.185 1738	−30.339 4198	20.981	0.402
3633	292.185 8386	−30.365 2012	20.082	0.414
3637	292.186 0246	−30.354 1686	21.078	0.458
4014	292.189 9276	−30.334 9827	20.018	0.163
4140	292.190 7422	−30.365 9681	20.510	0.458
4346	292.193 2713	−30.368 5683	20.874	0.462
4420	292.194 6120	−30.327 9961	21.127	0.435
4635	292.196 7567	−30.354 0156	19.512	0.203
4875	292.199 3316	−30.359 1077	21.066	0.413
5059	292.201 4691	−30.347 8313	22.921	0.668
5174	292.202 9316	−30.352 4965	20.789	0.421
5239	292.203 7376	−30.353 4943	20.504	0.282
5354	292.205 1005	−30.362 9483	21.345	0.428
5611	292.209 1052	−30.326 3457	20.941	0.382
5612	292.208 5462	−30.369 6267	21.149	0.460
6087	292.215 7226	−30.381 3623	20.019	0.238

Table 2. HB candidates. See Fig. 4 for the selection.

ID	α (2000.0)	δ(2000.0)	V	$B-V$
125	292.145 6946	−30.373 3031	17.819	0.331
370	292.149 3758	−30.347 7929	18.091	0.260
1127	292.158 6924	−30.365 8908	18.069	0.254
1549	292.164 1508	−30.335 2455	17.735	0.456
1996	292.169 0971	−30.351 9957	18.139	0.204
2040	292.169 1049	−30.382 8881	18.207	0.162
2086	292.170 1074	−30.348 4238	17.966	0.253
2503	292.174 6582	−30.337 7476	18.087	0.256
2608	292.175 3085	−30.365 9882	18.219	0.150
3036	292.180 2420	−30.330 2122	18.007	0.336
3038	292.180 2864	−30.328 0083	18.367	0.147
3129	292.180 7069	−30.365 6050	18.089	0.186
3204	292.181 5674	−30.358 9202	18.038	0.271
3555	292.184 8119	−30.383 2435	18.087	0.234
3682	292.186 4725	−30.358 2211	17.996	0.253
3772	292.187 1954	−30.365 1926	17.886	0.341
3990	292.189 4482	−30.353 4246	17.703	0.388
4040	292.189 8984	−30.353 3154	17.917	0.360
4911	292.199 8576	−30.347 6994	18.097	0.258
4932	292.200 2557	−30.335 2233	17.720	0.435
4940	292.199 7888	−30.374 8761	18.209	0.168
5048	292.201 1579	−30.355 2338	18.054	0.277
5101	292.201 9892	−30.350 1858	18.437	0.135
5165	292.203 3021	−30.320 8588	18.108	0.245
5184	292.202 9381	−30.359 9449	18.018	0.243
5244	292.203 8283	−30.354 4071	18.028	0.304
5646	292.208 7883	−30.386 3411	18.051	0.266
5773	292.211 5368	−30.328 9674	18.037	0.287

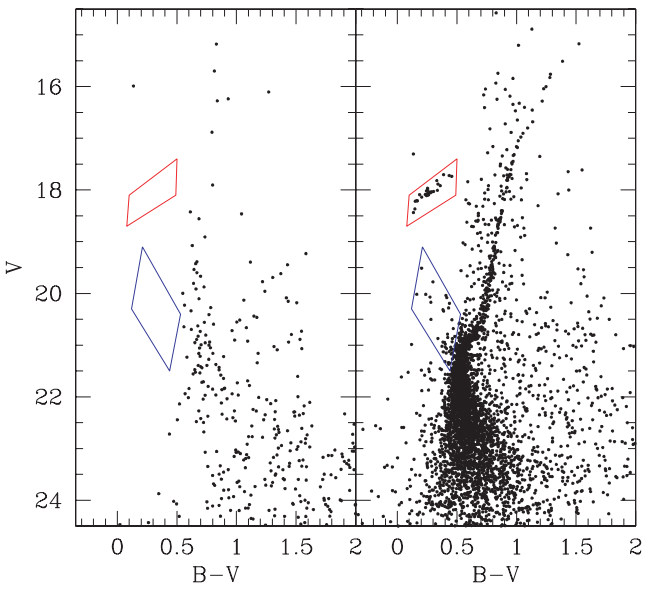

Figure 5. Estimate of field star contamination in Arp 2. The left-hand panel shows the Galaxy CMD in the Arp 2 direction, and the right-hand panel the CMD of Arp 2 as in Fig. 4.

6 DISCUSSION AND CONCLUSION

To better quantify the relationship between BSSs and the other stars, we make use of the Kolmogorov–Smirnov (KS) statistic, in its one- (1D) and two-dimensional (2D) flavours.

The 2D distributions of BSSs with respect to other star samples in different evolutionary phases (HB, RGB or MS stars) were statistically compared with the 2D generalization of the 1D KS test described in Press et al. (1997) and Fasano & Franceschini (1987). The same method was employed in Pancino et al. (2003) to compare the 2D distributions of RGB stars with different metallicities in the multipopulation globular cluster ω Cen.

This test gives probability (P) values which show that two distributions are extracted from the same parent distribution. Small values of P would mean that the two samples are significantly different. Formulae as given in Press et al. (1997) are accurate enough when

$$N = N_1 \times N_2/(N_1 + N_2) > 20 \quad (1)$$

and when the concerned probability P is less than (more significant than) 0.20 or so. In the above equation N_1 and N_2 are the two populations under comparison. When P is larger than 0.20, its value may not be accurate, but the implication that the two data sets are not significantly different is certainly correct. We summarize our results in Tables 3 and 4, and graphically in the series of Figs 7–9.

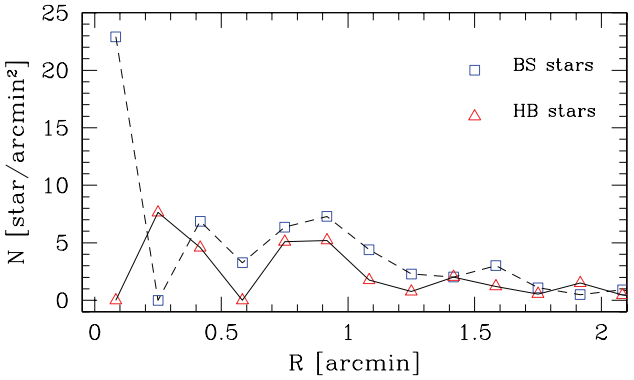

Figure 6. Radial surface density profile of HB (red triangles) and BSS (blue squares) stars in the field of Arp 2.

Table 3. Results of the KS statistics in 1D for BSSs.

Population	*N*	*P*	Reference figure
HB	17	0.83	Fig. 7
RGB	35	0.61	Fig. 8
MS	38	0.07	Fig. 9

Table 4. Results of the KS statistics in 2D for BSSs.

Population	*N*	*P*
HB	17	0.51
RGB	35	0.43
MS	38	0.23

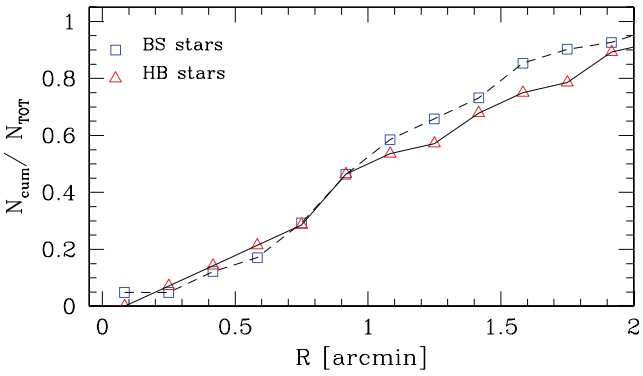

Figure 7. Fractional radial cumulative distribution of BSS and HB stars.

Looking at the results listed in the two tables and illustrated in the corresponding figures, we can provide the following considerations.

First, due to the larger number, the statistic (*N*) improves on passing from HB to RGB stars, and from RGB to MS stars.

Secondly, the probability *P* for the 2D KS test gives smaller values than for the 1D test in the case of HB and RGB stars. We face the opposite situation as for MS stars. We can explain it by taking into account the fact that the 1D distribution is only a function of the distance from the distribution centre, while 2D distributions do contain angle information. In the case of HB and RGB stars, radial distributions are very close to BSSs, while azimuthal distributions have some differences, and this results in larger probabilities in 1D testing. In the case of MS stars the radial distribution is very different from the BSS distribution, and probability in the 1D test

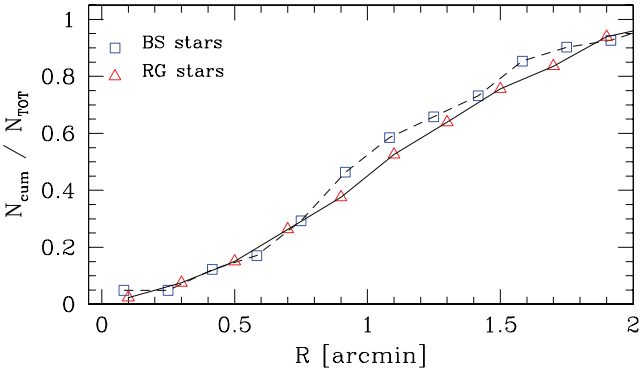

Figure 8. Fractional radial cumulative distribution of BSS and RGB stars.

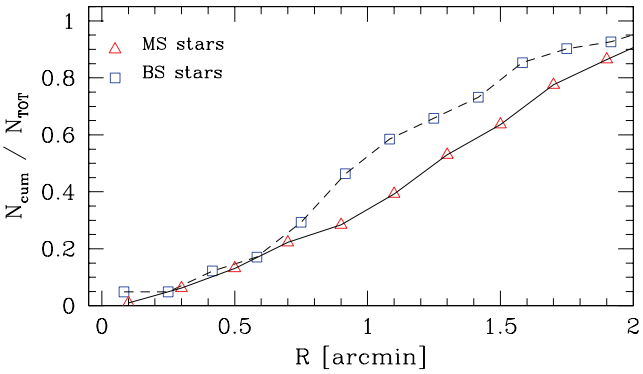

Figure 9. Fractional radial cumulative distribution of BSS and MS stars.

is small. Apparently, azimuthal distributions in this case are more similar, which implies a larger probability in the 2D test.

Thirdly, and more interesting, the tests provide comparable results for HB and RGB stars. This implies that BSS, HB and RGB stars are, overall, distributed in the same way, which in turn means that these populations are not significantly different. We caution, however, that a high probability in the KS test is a necessary, but not sufficient, condition to prove that these populations have the same parent distribution (see e.g. Press et al. 1997).

At odds with HB and RGB stars, MS stars show a different distribution when compared to BSSs. Namely, BSSs are significantly more concentrated to the cluster centre than normal MS stars. All considered, this suggests that most probably BSSs are primordial binary systems which, because of their total mass and the relatively loose environment of Arp 2, sank towards the centre and survived as binary systems.

Our results also imply that the present-day RGB and HB stars are, overall, more concentrated than actual MS stars. This does not mean that actual HB stars and upper RGB stars are more massive than actual MS stars, which can be the case for RGB stars in earlier stages of evolution. This simply reflects the fact that actual upper RGB and HB stars follow the spatial distribution of their – originally more massive – MS progenitors. The relaxation time for Arp 2 is ∼5 Gyr (Harris 1996), specifically much shorter than the cluster age, and therefore mass segregation already occurred in the past, when the progenitors of present-day upper RGB and HB stars were in the MS, and were more massive – and therefore more segregated – than the present-day MS stars.

Our findings confirm very recent results on the nature and distribution of BSSs in GCs (Ferraro et al. 2009).

Suggestions (Knigge et al. 2009) that most BSSs in globulars have a binary origin, even in the environment of the densest globulars, is no longer of general validity. In fact, whether BSSs are primordial close binaries or merger remnants resulting from direct collision between two stars depends strongly on the environment. As recently discovered by Ferraro et al. (2009), the existence of double BSS sequences in M30, a famous *core collapse* globular cluster, confirms that the nature of BSSs depends strongly on the environment, and on the dynamical state of the parent cluster.

Loose systems, such as open clusters, do indeed show a high primordial binary fraction among their BSSs (Sandquist 2005; Mathieu & Gheller 2009), while very dense systems harbour both primordial binaries and merger products, in proportions that vary from cluster to cluster.

In this context, Arp 2 is a relatively low concentration globular that follows this trend, which will be hopefully confirmed by future spectroscopic observations.

ACKNOWLEDGMENTS

GC expresses his gratitude to O. Hainaut and G. Lo Curto for assistance during the observations, and Y. Momany for long useful conversations on blue stragglers. We express special thanks to the referee, Robert Rood, for the careful reading and useful suggestions he provided. Finally, we express our gratitude to Sandy Strunk for reading the manuscript carefully and improving the language. In the preparation of this paper, we made use of the NASA Astrophysics Data System and the Astro-ph e-print server. This work made extensive use of the SIMBAD data base, operated at the CDS, Strasbourg, France.

REFERENCES

Ahumada J. A., Lapasset E., 1995, A&A, 109, 375
Ahumada J. A., Lapasset E., 2007, A&A, 463, 789
Buonanno R., Corsi C. E., Fusi Pecci F., Fahlman G. G., Richer H. B., 1994, ApJ, 430, L121
Carraro G., Zinn R., Moni Bidin C., 2007, A&A, 466, 181
Dalessandro E., Lanzoni B., Ferraro F. R., Vesperini F., Bellazzini M., Rood R. T., 2008a, ApJ, 681, 311
Dalessandro E., Lanzoni B., Ferraro F. R., Rood R. T., Milone A., Piotto G., Valenti E., 2008b, ApJ, 677, 1069
Davies M., Piotto G., de Angeli F., 2004, MNRAS, 349, 129
Fasano G., Franceschini A., 1987, MNRAS, 225, 155
Ferraro F. R., Fusi Pecci F., Cacciari C., Corsi C., Buonanno R., Fahlam G. G., Richer H. B., 1993, AJ, 106, 2324
Ferraro F., 2006, in Modelling Dense Stellar Systems, 26th meeting of the IAU, JD14, 4
Ferraro F. R. et al., 2009, Nat, 462, 24
Girardi L., Groenewegen M. A. T., Hatziminaoglou E., da Costa L., 2005, A&A, 436, 895
King I., 1962, AJ, 67, 471
Harris W. E., 1996, AJ, 112, 1487
Knigge C., Leigh N., Sills A., 2009, Nat, 457, 15
Layden A. C., Sarajedini A., 2000, AJ, 119, 1760
Landolt A. U., 1992, AJ, 104, 372
Lanzoni B., Dalessandro E., Ferraro F. R., Mancini C., Beccari G., Rood R. T., Mapelli M., Sigurdsson S., 2007, ApJ, 663, 267
Liu G. Q., Deng L., Chávez M., Bertone E., Herreo Davo A., Mata-Chávez M. D., 2008, MNRAS, 390, 665
Mathieu R. D., Gheller A. M., 2009, Nat, 462, 24
Monaco L., Bellazzini M., Bonifacio P., Ferraro F. R., Marconi G., Pancino E., Sbordone L., Zaggia S., 2005, A&A, 441, 141
Mottini M., Wallerstein G., McWilliam A., 2008, AJ, 136, 614
Pancino E., Seleznev A., Ferraro F. R., Bellazzini M., Piotto G., 2003, MNRAS, 345, 683
Patat F., Carraro G., 2001, MNRAS, 325, 1591
Perets H. B., Fabrycky D. C., 2009, ApJ, 697, 1048
Press W. H., Teukolsky S. A., Vetterling W. T., Flannery B. P., 1997, The Art of Scientific Computing, 2nd edn. Cambridge Univ. Press, New York
Sandage A. R., 1953, AJ, 58, 61
Sandquist E. L., 2005, ApJ, 635, L73
Seleznev A. F., 1994, A&A, 4, 167
Stetson P. B., 1987, PASP, 99, 191

This paper has been typeset from a TEX/LATEX file prepared by the author.